

# Simple buffers for 3D STORM microscopy

Nicolas Olivier,<sup>1,\*</sup> Debora Keller,<sup>2</sup> Vinoth Sundar Rajan,<sup>1</sup>  
Pierre Gönczy,<sup>2</sup> and Suliana Manley<sup>1</sup>

<sup>1</sup>Laboratory for Experimental Biophysics, School of Basic Sciences, Swiss Federal Institute of Technology (EPFL), CH-1015 Lausanne, Switzerland

<sup>2</sup>Swiss Institute for Experimental Cancer Research (ISREC), School of Life Sciences, Swiss Federal Institute of Technology (EPFL), CH-1015 Lausanne, Switzerland

\* [nicolas.olivier@polytechnique.edu](mailto:nicolas.olivier@polytechnique.edu)

**Abstract:** 3D STORM is one of the leading methods for super-resolution imaging, with resolution down to 10 nm in the lateral direction, and 30-50 nm in the axial direction. However, there is one important requirement to perform this type of imaging: making dye molecules blink. This usually relies on the utilization of complex buffers, containing different chemicals and sensitive enzymatic systems, limiting the reproducibility of the method. We report here that the commercial mounting medium Vectashield can be used for STORM of Alexa-647, and yields images comparable or superior to those obtained with more complex buffers, especially for 3D imaging. We expect that this advance will promote the versatile utilization of 3D STORM by removing one of its entry barriers, as well as provide a more reproducible way to compare optical setups and data processing algorithms.

© 2013 Optical Society of America

**OCIS codes:** (180.0180) Microscopy; (180.2520) Fluorescence microscopy; (180.6900) Three-dimensional microscopy; (100.6640) Superresolution; (170.3880) Medical and biomedical imaging.

## References and links

1. E. Betzig, G. H. Patterson, R. Sougrat, O. W. Lindwasser, S. Olenych, J. S. Bonifacino, M. W. Davidson, J. Lippincott-Schwartz, and H. F. Hess, "Imaging intracellular fluorescent proteins at nanometer resolution," *Science* **313**, 1642–1645 (2006).
2. S. T. Hess, T. P. Girirajan, and M. D. Mason, "Ultra-high resolution imaging by fluorescence photoactivation localization microscopy," *Biophys. J.* **91**, 4258–4272 (2006).
3. M. J. Rust, M. Bates, and X. Zhuang, "Sub-diffraction-limit imaging by stochastic optical reconstruction microscopy (STORM)," *Nat. Methods* **3**, 793–796 (2006).
4. M. Heilemann, E. Margeat, R. Kasper, M. Sauer, and P. Tinnefeld, "Carbocyanine dyes as efficient reversible single-molecule optical switch," *J. Am. Chem. Soc.* **127**, 3801–3806 (2005).
5. M. Bates, T. R. Blosser, and X. Zhuang, "Short-range spectroscopic ruler based on a single-molecule optical switch," *Phys. Rev. Lett.* **94**, 108101 (2005).
6. M. Heilemann, S. van de Linde, M. Schüttelpelz, R. Kasper, B. Seefeldt, A. Mukherjee, P. Tinnefeld, and M. Sauer, "Subdiffraction-resolution fluorescence imaging with conventional fluorescent probes," *Angew. Chem. Int. Ed.* **47**, 6172–6176 (2008).
7. G. T. Dempsey, M. Bates, W. E. Kowtoniuk, D. R. Liu, R. Y. Tsien, and X. Zhuang, "Photoswitching mechanism of cyanine dyes," *J. Am. Chem. Soc.* **131**, 18192–18193 (2009).
8. C. Steinhauer, C. Forthmann, J. Vogelsang, and P. Tinnefeld, "Superresolution microscopy on the basis of engineered dark states," *J. Am. Chem. Soc.* **130**, 16840–16841 (2008).
9. S. Van De Linde, A. Löschberger, T. Klein, M. Heidbreder, S. Wolter, M. Heilemann, and M. Sauer, "Direct stochastic optical reconstruction microscopy with standard fluorescent probes," *Nat. Protoc.* **6**, 991–1009 (2011).

10. X. Shi, J. Lim, and T. Ha, "Acidification of the oxygen scavenging system in single-molecule fluorescence studies: in situ sensing with a ratiometric dual-emission probe," *Anal. Chem.* **82**, 6132–6138 (2010).
11. J. Vogelsang, T. Cordes, and P. Tinnefeld, "Single-molecule photophysics of oxazines on DNA and its application in a FRET switch," *Photochem. Photobiol. Sci.* **8**, 486–496 (2009).
12. T. Dertinger, R. Colyera, G. Iyer, S. Weiss, and J. Enderlein, "Fast, background-free, 3D super-resolution optical fluctuation imaging (SOFI)," *Proc. Natl. Acad. Sci. U.S.A.* **106**, 22287–22292 (2009).
13. S. J. Holden, S. Uphoff, and A.N. Kapanidis, "DAOSTORM: an algorithm for high-density super-resolution microscopy," *Nat. Methods* **8**, 279–280 (2011).
14. S. Cox, E. Rosten, J. Monypenny, T. Jovanovic-Taliman, D. T. Burnette, J. Lippincott-Schwartz, G. E. Jones, and R. Heintzmann, "Bayesian localization microscopy reveals nanoscale podosome dynamics," *Nat. Methods* **9**, 195–200 (2012).
15. T. Cordes, A. Maiser, C. Steinhauer, L. Schermelleh, and P. Tinnefeld, "Mechanisms and advancement of anti-fading agents for fluorescence microscopy and single-molecule spectroscopy," *Phys. Chem. Chem. Phys.* **13**, 6699–6709 (2011).
16. L. Schermelleh, P. M. Carlton, S. Haase, L. Shao, L. Winoto, P. Kner, B. Burke, M. C. Cardoso, D. A. Agard, M. G. L. Gustafsson, H. Leonhardt, and J. W. Sedat, "Subdiffraction multicolor imaging of the nuclear periphery with 3D structured illumination microscopy," *Science* **320**, 1332–1336 (2008).
17. B. Huang, W. Wang, M. Bates, and X. Zhuang, "Three-dimensional super-resolution imaging by stochastic optical reconstruction microscopy," *Science* **319**, 810–813 (2008).
18. B. Huang, S. A. Jones, B. Brandenburg, and X. Zhuang, "Whole-cell 3D STORM reveals interactions between cellular structures with nanometer-scale resolution," *Nat. Methods* **5**, 1047–1052 (2008).
19. E. Nogales, and G. Alushin, "4.6 Tubulin and microtubule structure: mechanistic insights into dynamic instability and its biological relevance," in *Comprehensive Biophysics*, E. H. Egelman, ed. (Elsevier, 2012), pp. 72–92.
20. R. E. Thompson, D. R. Larson, and W. W. Webb, "Precise nanometer localization analysis for individual fluorescent probes," *Biophys. J.* **82**, 2775–2783 (2002).
21. G. Dempsey, J. Vaughan, K. Chen, M. Bates, and X. Zhuang, "Evaluation of fluorophores for optimal performance in localization-based super-resolution imaging," *Nat. Methods* **8**, 1027–1036 (2011).
22. K. Valnes and P. Brandtzaeg, "Retardation of immunofluorescence fading during microscopy," *J. Histochem. Cytochem.* **33**, 755–761 (1985).
23. J. Widengren, A. Chmyrov, C. Eggeling, P. Löfdahl, and C. A. M. Seidel, "Strategies to improve photostabilities in ultrasensitive fluorescence spectroscopy," *J. Phys. Chem. A* **111**, 429–444 (2007).
24. M. F. Juette, T. J. Gould, M. D. Lessard, M. J. Mlodzianoski, B. S. Nagpure, B. T. Bennett, S. T. Hess, and J. Bewersdorf, "Three-dimensional sub-100 nm resolution fluorescence microscopy of thick samples," *Nat. Methods* **5**, 527–529 (2008).
25. G. Shtengel, J. A. Galbraith, C. G. Galbraith, J. Lippincott-Schwartz, J. M. Gillette, S. Manley, R. Sougrat, C. M. Waterman, P. Kanchanawong, M. W. Davidson, R. D. Fetter, and H. F. Hess, "Interferometric fluorescent super-resolution microscopy resolves 3D cellular ultrastructure," *Proc. Natl. Acad. Sci. U.S.A.* **106**, 3125–3130 (2009).
26. T. Staudt, M. C. Lang, R. Medda, J. Engelhardt, and S. W. Hell, "'2,2'-Thiodiethanol: A new water soluble mounting medium for high resolution optical microscopy" *Microsc. Res. Tech.* **70**, 1–9 (2006).
27. J. Fölling, V. Belov, R. Medda, A. Schönle, A. Egner, C. Eggeling, M. Bossi, and S. W. Hell, "Photochromic rhodamines provide nanoscopy with optical sectioning," *Angew. Chem. Int. Ed.* **46**, 6266–6270 (2007).
28. P. Gönczy, "Towards a molecular architecture of centriole assembly," *Nat. Rev. Mol. Cell Biol.* **13**, 425–435 (2012).
29. S. Lawo, M. Hasegan, G. D. Gupta, and L. Pelletier, "Subdiffraction imaging of centrosomes reveals higher-order organizational features of pericentriolar material," *Nat. Cell Biol.* **14**, 1148–1158 (2012).
30. I. H. Stein, S. Capone, J. H. Smit, F. Baumann, T. Cordes, and P. Tinnefeld, "Linking single-molecule blinking to chromophore structure and redox potentials," *ChemPhysChem* **13**, 931–937 (2012).
31. A. Lampe, V. J. Haucke, S. Sigris, M. Heileman, and J. Schmoranz, "Multi-colour direct STORM with red emitting carbocyanines," *Biol. Cell* **104**, 229–237 (2012).

---

## 1. Introduction

Super resolution microscopy relying on the localization of individual fluorescent molecules [1–3] requires them to be fluorescent only a fraction of the time so that they can be localized individually. This temporal separation can be achieved by using an intrinsic optical switch, for example a photo-switchable/photo-activatable fluorescent protein or an uncageable dye [1, 2]. Alternatively, reversible blinking can be induced with standard fluorescent dyes by the addition of chemicals in the imaging buffer which influence their photophysical properties [3–6]. The mechanism behind chemically induced blinking has been identified for a few dyes [7],

and is due to the presence of a long lived non-fluorescent state, which can be accessed in theory by any fluorescent dye [8]. Indeed, blinking of many fluorophores, including commonly used cyanine and rhodamine dyes, has already been reported, as reviewed for example in [9]. Stochastic optical reconstruction microscopy (STORM) imaging buffers are usually made of several chemicals, and in particular rely on an enzymatic oxygen scavenging system to remove oxygen, which is the main source of photobleaching. The most widely used system, which consists of glucose and the two enzymes glucose oxidase and catalase leads to significant buffer acidification over time [10], which affects the photophysics of dyes [11], and thus limits the reproducibility of the method. This implies that buffers must be freshly prepared for each experiment, and that their lifetime is limited to a few hours at most. Moreover, some of the chemicals used (mercaptoethanol, methyl viologen) are highly toxic, limiting their use in standard microscope rooms.

While several alternative super-resolution methods have recently been developed to bypass the stringent requirements of single-molecule imaging [12–14], the quality of the images obtained still depends on the quality of the blinking. For instance, Stochastic Optical Fluctuation Imaging (SOFI) [12] does not rely on single molecule localization but still makes use of the temporal fluctuations in the fluorescence intensity, thereby improving the resolution compared to confocal microscopy about 2-5 fold, depending on the amplitude of the modulation. Thus, increasing the robustness and effectiveness of blinking buffers is an important aspect of improving the accessibility and quality of all blinking-based super-resolution methods.

Vectashield is a commercially available anti-fading mounting medium, whose anti-fading mechanism was recently studied at the single molecule level [15]. Vectashield is a glycerol-based medium, whose high optical index makes it convenient for high numerical aperture (NA) imaging. It is also a non-hardening medium that can maintain samples for up to several weeks at 4°C. Due to its ability to limit photobleaching, it has been used as an imaging medium for 3D Structured Illumination Microscopy (3D-SIM) [16]. Vectashield is not recommended for every fluorophore, though, since the anti-fading chemicals can have a negative influence on the stability of some dyes. Indeed, it has been reported that the dye Cy2 should not be used in Vectashield due to reduced fluorescence relative to that in PBS. We show here that Vectashield is highly beneficial for STORM imaging of a subset of dyes, as it induces prolonged blinking and enables the generation of high-quality super resolution STORM images. In particular, we demonstrate this for Alexa-647, which is the most widely used dye for STORM imaging, and show that this buffer allows us to improve 3D imaging by index-matching. In addition we screened a number of dyes across the optical spectrum and marking microtubules to assess STORM buffers containing Vectashield and thus identified suitable multicolor combinations.

## 2. Materials and methods

### 2.1. Optical setup

Imaging was performed on a modified Olympus IX71 inverted microscope. Lasers at 641 nm (Coherent, CUBE 640-100C) 488 nm (Coherent Sapphire), and 561 nm (Coherent Sapphire) were reflected by a multiband dichroic (89100bs, Chroma) onto the back aperture of a 100x 1.3 NA oil objective (Olympus, UplanFL) mounted on a piezo objective scanner (P-725 PIFOC, Physik Instrumente). The collected fluorescence from the sample was filtered using a band-pass emission filter (ET700/75, ET600/75 and ET525/50, all Chroma), for far-red dyes, red dyes and green dyes respectively) and imaged onto an EMCCD camera (IxonEM+, Andor) with a 100 nm pixel size and using the conventional CCD amplifier at a frame rate of 25 frames per second. Laser intensity on the sample was  $\approx 1\text{-}2\text{ kW}\cdot\text{cm}^{-2}$  and 10,000-20,000 frames were typically recorded for a total imaging time of  $\approx 6\text{-}12$  minutes.

For 3D imaging, a cylindrical lens ( $f = 1000$  mm, Thorlabs LJ1516RM-A) was added to

the imaging path to enable the z-localization of fluorophores via astigmatic shaping of the point spread function [17], using one arm of an Optosplit system (CAIRN) and placing the cylindrical lens at the position typically occupied by the fluorescence filter, which is close to the Fourier plane.

## 2.2. Sample preparation

African green monkey kidney cells COS-7 were cultured in DMEM supplemented with 10% FBS (Sigma-Aldrich Aldrich) in a cell culture incubator (37°C and 5% CO<sub>2</sub>) and plated at low confluency on cleaned 25 mm size 1 cover-glass (Menzell). Prior to fixation, all solutions were pre-warmed at 37°C: 24 hours after plating, cells were pre-extracted for 10 s in 0.5% Triton X-100 (Triton) in BRB80 (80 mM PIPES, 1 mM MgCl<sub>2</sub>, 1 mM EGTA, adjusted to pH 6.8 with KOH) supplemented with 4 mM EGTA, washed in PBS, fixed for 10 min in -20°C-Methanol (Sigma-Aldrich), and washed again in PBS. The samples were then blocked 30 minutes in 5% BSA, before being incubated for 1.5h at room temperature with 1:1000 mouse alpha-tubulin antibodies (Sigma-Aldrich, T5168) in PBS - 1% BSA - 0.2% Triton (PBST), followed by 3 washes with PBS-0.2% Triton, and then incubated for 45min in PBST with 1:1000 goat anti-mouse Alexa-647 F(ab)<sub>2</sub> secondary antibody fragments (Life Technologies, A-21237).

For the dye screening, the same protocol was used except the Alexa Fluor 647 secondary antibody was replaced by: Alexa-488 (Life Technologies, A-10684), Alexa-532 (Life Technologies, A-11002), Alexa-555 (Life Technologies, A-21425), Alexa-546 (Life Technologies, A-11018), Alexa-568 (Life Technologies, A-11019), Alexa-700 (Life Technologies, A-21036), Cy3 (Jackson ImmunoResearch, 115-165-146), Cy3.5 (Abcam, 97036), Cy5 (Life Technologies, M35011), CF-488 (Biotium, 20011), CF-647 (Biotium, 20281), Rhodamine-6G (ActiveMotif, 15075), Flip-565 (Abberior, 2-0002-202-4), and Atto-655 (Sigma-Aldrich-Aldrich 50283). For Cy3B (GE, PA06310) we directly conjugated the dye to a primary antibody (Sigma-Aldrich, T5168). Dy-647 was tested on cells transiently expressing SNAP-EB3, and incubated after fixation with BG-Dy647 (NEB S9137S).

For CEP-152 imaging, U2OS cells (European Collection for Cell Cultures) were maintained in McCoy's 5A GlutaMAX medium (Life Technologies) supplemented with 10% FBS in a cell culture incubator (37°C and 5% CO<sub>2</sub>) and plated at low confluency on cleaned 25 mm size 1 cover-glass (Menzell). Fixation and immunostaining was performed similarly as for tubulin, except that the primary antibody used was anti-CEP152 produced in rabbit (Sigma-Aldrich, HPA039408) at 1:2000 in PBST, and the secondary antibody was Goat anti-rabbit Cy3 (Jackson ImmunoResearch, 111-165-144) at 1:1000 in PBST.

Imaging was performed by placing the 25 mm coverslip into a holder, then pipetting 30  $\mu$ L of Vectashield (Vectorlab, H-1000) on top of it and adding a clean 18 mm coverslip to spread the Vectashield evenly. Alternatively, we used a mixture of Vectashield and 95% Glycerol - 50 mM TRIS pH8 (referred to hereafter as TRIS-Glycerol) obtained by adding 5% v/v TRIS 1 M pH 8 in Glycerol, or more complex buffers described below. After imaging, coverslips were briefly washed in PBS to remove residual Vectashield and kept in PBS containing antibiotics at 4°C until further imaging.

Propyl Gallate (NPG) (Sigma-Aldrich, P3130) was prepared as a stock solution of Glycerol-NPG using 5% w/v NPG in 90% Glycerol, 10% v/v TRIS, pH 8. DABCO (Sigma-Aldrich, D27802) was prepared as a 1 M solution in TRIS and used to create a stock solution of Glycerol-DABCO (100 mM in 90% Glycerol, 10% TRIS, pH 8). alpha-Lipoic Acid ( $\alpha$ LA) (Sigma-Aldrich, 62320) was prepared as a 1M stock solution in TRIS 10% Ethanol (v/v) and then diluted to create a stock solution of Glycerol- $\alpha$ LA (100 mM in 90% Glycerol, 10% TRIS, pH 8). Thiodiglycol (2,2-thiodiethanol or TDE, Alfa Aesar, A17002) was mixed v/v with pure Vectashield.

Vectashield absorption and emission spectra were measured on a fluorescence spectrometer (Jasco FP-8500) using  $\approx 1$  mL of pure Vectashield in a 10 mm fluorescence cuvette. Absorption was first measured from 300 nm to 700 nm, and emission was measured at 3 wavelengths close to the imaging wavelengths used: 405 nm, 560 nm and 630 nm, all with a 5 nm spectral width.

### 2.3. Data analysis

#### 2.3.1. 2D imaging

Each peak with a high enough signal-to-noise ratio was fitted to a Gaussian function by non-linear least-square fitting, and positions as well as photon counts were extracted from the fitted peaks for rendering and quantification purposes (Peakselector, courtesy of H. Hess). Peaks detected for more than 15 consecutive frames, as well as peaks localized with fewer than 1500 photons for Alexa 647, or 500 photons for the other dyes tested were removed from the analysis. Peaks detected in successive frames at a distance of less than 40 nm were considered as originating from a single molecule and grouped (see paragraph below for grouping details).

Grouping of localizations in successive frames was performed using Matlab. Localized peaks were tracked in 2d (x-y) using a single particle tracking algorithm (<http://physics.georgetown.edu/matlab/index.html>) with a search radius of 40 - 50 nm, and all localizations in a single track were averaged to give a final molecular localization, and summed to give a molecular number of photons. The standard deviations of the x, y, (and z) positions were also calculated for each track containing between 5 and 15 points and used as a measure of localization precision. Molecules displaying unusually large standard deviations in z (typically, bigger than 40 nm) were discarded from the analysis. Drift correction was performed using Peakselector by measuring the mean vertical (resp horizontal) position of a straight horizontal (resp vertical) segment of microtubules as a function of frame number, performing a moving average over this function (moving average over 1000 frames), and subtracting the fitted function from the vertical (resp horizontal) coordinates of all the peaks.

The data was rendered using Matlab ('hist3' function) to bin the localizations in a 10 nm per pixel grid, and then a Gaussian blur of  $\sigma = 5$  nm was added to obtain a smoother rendering using ImageJ ([rsb.info.nih.gov/ij/](http://rsb.info.nih.gov/ij/)).

#### 2.3.2. 3D imaging

For 3D STORM, the width and height of the image of a single emitter as a function of depth was calibrated using fluorescent beads, according to [17, 18]. Briefly, images of  $\approx 10$  beads were recorded at intervals of 20 nm using the objective piezo scanner, and fitted with an elliptical Gaussian function using Peakselector. The width vs. depth and height vs. depth of each bead was then fitted with a model function [17] (Eq. (1) with  $w_0$ , A, B, c and d as free parameters) using Matlab's "fit" function and the fit parameters for the different beads were averaged to give a calibration curve.

$$w_x(z) = w_0 * \sqrt{1 + ((x - c)/d)^2 + A((x - c)/d)^3 + B((x - c)/d)^4} \quad (1)$$

Using this calibration data, we then created a z-position look-up-table relating width and height to z position for every combination of width ( $w_x^i$ ) and height ( $w_y^j$ ) in a given range ( $[wx_{min} : dw : wx_{max}]$ ,  $[wy_{min} : dw : wy_{max}]$ ) by minimizing in z the distance  $M(z)^{i,j}$  between each height-width couple ( $w_x^i, w_y^j$ ) and the calibration data ( $w_x(z), w_y(z)$ ) according to Eq. (2) [17] with Matlab's "fminsearch" function. The resulting minimum value  $M_{min}$  was then used as a goodness of fit and saved in another look-up-table.

$$M(z) = \left( \sqrt{wx_m} - \sqrt{w_x(z)} \right)^2 + \left( \sqrt{wy_m} - \sqrt{w_y(z)} \right)^2 \quad (2)$$

Finally, this z-position look-up-table was used to convert the measured width and height parameters from the fitted peaks into a z-coordinate. Peaks localized with a goodness of fit higher than a user-defined threshold (the lower the threshold, the higher the localization precision, but the lower the density) were discarded from the analysis (for the 3D image shown in section 3.2, around 10% of the localized peaks were discarded in this step). The data was then grouped using Matlab, and the final localizations were rendered using Peakselector, with the depth color-coded. Total processing time was  $\approx 10$  minutes per image.

### 3. Results

#### 3.1. 2D imaging

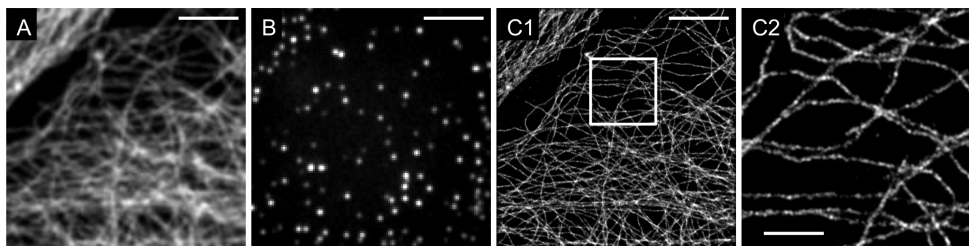


Fig. 1. STORM imaging of microtubules (see section 2.2 for more details) in Vectashield. (A): Widefield image (B): Single frame, (C1): Reconstructed STORM image, with blow-up on the ROI in (C2). scale-bar = 5  $\mu\text{m}$  for (A),(B),(C1) and 1  $\mu\text{m}$  for C2.

In eukaryotic cells, microtubules form extended polymer networks from dimers of  $\alpha$ - and  $\beta$ - tubulin. Each microtubule is a polymer tube of 25 nm in outer diameter [19], well below the diffraction limit. To test Vectashield as a STORM buffer for Alexa-647, we used as a test-sample fixed cells in which microtubules were immunostained with primary antibodies against  $\alpha$ -tubulin and with secondary antibody fragments labeled with Alexa-647 (see Section 2.2). We then simply added Vectashield (see Section 2.2) turned on our excitation laser to full power ( $\approx 1.5 \text{ kW}\cdot\text{cm}^{-2}$ ) and recorded 10,000 frames. Figure 1 shows a typical dataset, with Fig. 1(A) showing an image reconstructed by projecting the mean frame intensity, and subtracting from it the projected minimum pixel intensity, yielding an image which is similar to a widefield image. After an initial bleaching step lasting a few frames (typically 10-20), single molecule blinking could be observed, as shown in Fig. 1(B) where we display the raw data captured in frame 2500. A sparse population of dyes can be seen in the fluorescent state, as is required to localize them individually. We reconstructed a STORM image (Fig. 1(C1)) from all localized molecules (according to Section 2.3) with a higher magnification view given in Fig. 1(C2) Since there is high temporal variability in the fluorescence signal, this data could also be processed with a SOFI [12] algorithm, and would yield an image of resolution intermediate between the STORM and the widefield images.

Having established that Vectashield can be used to generate STORM images, we wanted to quantify several features reflecting its quality as a bona-fide STORM buffer. The quality of a buffer depends mainly on three parameters:

1. The brightness of each molecule, since the localization precision scales as the square root of the number of detected photons [20]. This value can be extracted directly from the raw data.
2. The blinking properties of each dye: the dye needs to have a long OFF state compared to its ON state to fulfill the single molecule localization constraints, but should not irreversibly photobleach, since this will result in a lower density of localizations.
3. The control over the density of molecules: this parameter is the hardest to quantify, since single molecule measurements are performed on very sparse samples where identifying single molecules is easy. However, for STORM imaging, the single molecule requirements depend strongly on the density of dyes in the sample, so the ideal buffer should be tunable enough to permit single molecule localizations for different densities.

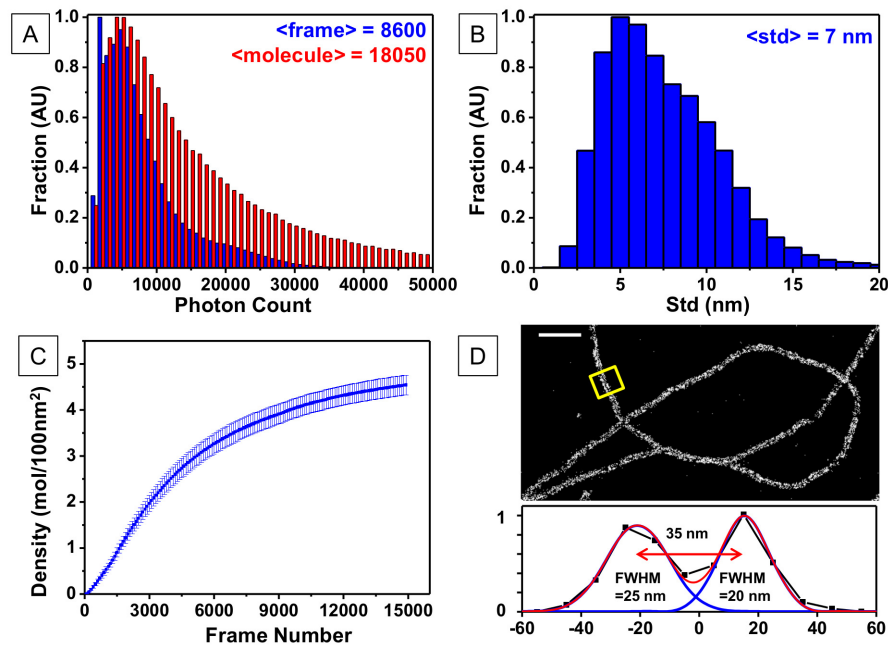


Fig. 2. Quantifying the quality of Vectashield as a STORM buffer for Alexa-647: (A) photon count distribution per frame (blue) and per molecule (red), obtained by grouping consecutive frame localizations and (B) standard deviation of multiple localizations (see section 2.3 for grouping details), with mean values displayed in the top right corner (C) Density of molecules as a function of number of recorded frames, averaged over three measurements. The error bar indicates the standard deviation. (D) STORM image of microtubule, on which the hollowness of the structure can be resolved, as quantified in the profile taken over the 200 nm yellow-boxed region with  $\approx 35$  nm between the two peaks, consistent with a 25 nm structure broadened by the antibodies.

Single molecule brightness was extracted from the fits to the raw data as described in section 2.3. ON and OFF times can be assessed by performing *in vitro* single-molecule analysis [21] but we chose instead to focus on the end result - the reconstituted STORM image - as an indirect measure of the blinking properties as well as the density (and therefore circumvent issues with translating *in vitro* measures). If the buffer is suitable, then the localization precision and density of molecules should be sufficient to reconstruct a high quality image.

Figure 2 represents the measured parameters used to evaluate Vectashield as a STORM buffer for Alexa-647. First, we directly measured the number of detected photons per molecule (Fig. 2(A), mean value of 18050 photons), as well as the standard deviation of repeated localizations of the same molecule (Fig. 2(B), mean value of 7 nm) which is less direct because it depends on the brightness of the molecule, but also on the background level, pixel size and fitting algorithm used. According to both of these measures, Vectashield compares positively with previously reported values, with mean photon counts per molecule usually in the 5,000-10,000 range [3, 6]. It is important to note that the standard deviation corresponds to the localization precision per frame, and that the expected localization precision per molecule will scale as the standard error of the mean. Since molecules are ON for an average of  $\approx 2 - 3$  frames, the localization precision for grouped molecules is expected to be  $\approx 40 - 70\%$  better than the standard deviation displayed. In our hands, the improvement over the commonly used Cysteamine + glucose oxidase + catalase buffer in terms of photon count is  $\approx 2$ , with a corresponding 40% increase in mean localization precision at the cost of a more limited control over the blinking.

To examine the time-dependence of dye photoswitching, we plotted in Fig. 2(C) the density of molecules on the structure (see section 2.3). The limitation of this measure is that it is sample-dependent since it varies with the structure imaged, but nevertheless it shows a constant increase in the cumulative density of localizations after an initial transient phase, indicating a steady blinking of Alexa-647 molecules over the duration of the measurement. Finally, we rendered the resultant STORM image (Fig. 2(D)) of microtubules immunostained with primary antibodies against  $\alpha$ -tubulin and with secondary antibody fragments labeled with Alexa-647. Microtubules are hollow tubes 25 nm in diameter [19], whose size is increased by the antibodies that target their exterior surface. STORM imaging in Vectashield allows that hollowness to be resolved, as can be seen from the lateral profile taken over a 200 nm region showing a clear double peak, with a separation distance of 35 nm (Fig. 2(D), bottom panel). This hollow structure has until now only been observed using full-length antibodies and the best known dye/buffer combination [21], demonstrating that Vectashield is indeed a very good buffer for STORM imaging using Alexa-647.

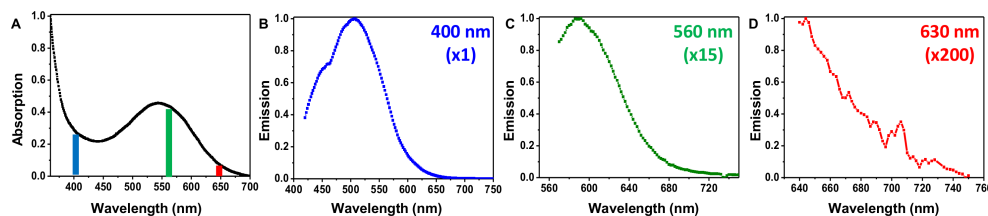


Fig. 3. (A) Absorption spectrum of Vectashield, as well as normalized emission spectra measured at 3 different wavelengths: 400 nm (B), 560 nm (C) and 630 nm (D) with normalization factor indicated in the top right corner.

Vectashield appears as a violet-colored medium, and therefore could potentially be auto-fluorescent, so because very high laser powers are used for STORM this could lead to high background and therefore decreased SNR and image resolution. To better quantify this potential limitation, we measured the absorption and emission spectra of Vectashield. The absorption spectrum (Fig. 3(A)) shows two broad absorption peaks: one in the UV ( $\approx 350$  nm), and one in the green ( $\approx 540$  nm). Emission spectra were measured for three excitation wavelengths: 630 nm, 400 nm (which is often used in STORM imaging to accelerate the rate of recovery from the dark state [9]), and 560 nm, which could be used for multicolor imaging. 400 nm light excited strong fluorescence emission over a broad spectrum, indicating that the use of UV light should be minimized. Therefore, all images shown in the article were acquired without using any UV

to re-activate dyes. The emission spectrum obtained using 560 nm excitation show significant (though  $\approx 15$  times weaker than that measured at 400 nm) fluorescence emission centered around 600 nm, which means that imaging in the red channel with Vectashield would suffer from elevated background levels. Finally, the emission spectrum obtained at 630 nm shown in Fig 3(D) showed only weak ( $\approx 200$  times weaker than at 400 nm) fluorescence, which does not interfere with imaging (as shown in Figs. 1 and 2) but does increase the background slightly.

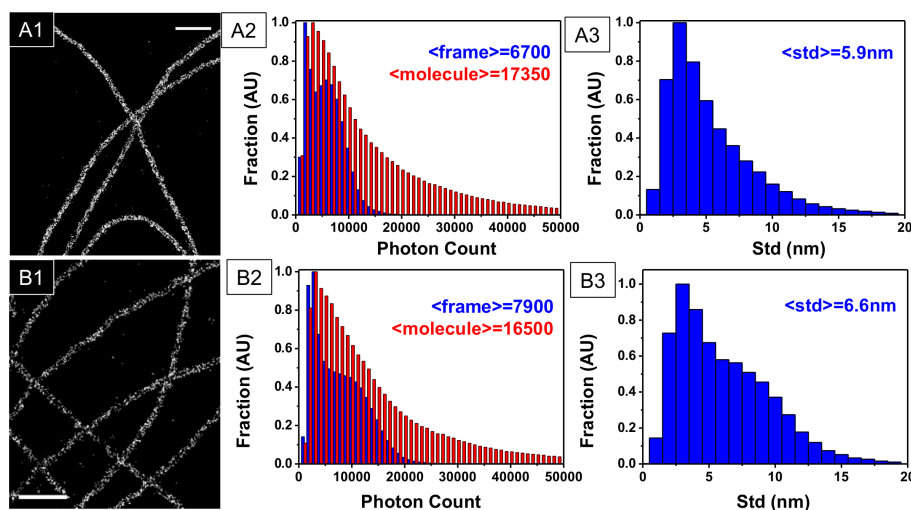


Fig. 4. STORM imaging of Alexa-647 stained microtubules in a Vectashield/TRIS-Glycerol mixture: (A) 50% Vectashield and (B) 25% Vectashield. The different panels represent: (1) STORM image reconstructed from 15,000 frames, scale-bar = 500 nm (2) photon count distribution per frame and per molecule, averaged over three data-sets, and (3) standard deviation of multiple localizations giving a measure of the frame localization precision.

One way to limit the influence of autofluorescence is to dilute Vectashield in a non-fluorescent medium. Indeed, we found that Vectashield can be diluted 1:1 (50% Vectashield) or 1:4 (25% Vectashield) in a TRIS-Glycerol solution (see section 2.2) without impairing dye blinking (Figs. 4(A) and 4(B)), yielding similar values as for pure Vectashield (compare with Fig. 2) while reducing fluorescence (by a factor  $\approx 6$  for a 4x dilution). This weak dependence on working concentration is reminiscent of the properties of thiol-based buffers, where concentrations ranging from 1-100 mM have been reported as effective [9, 21].

This mixing opens interesting possibilities for further manipulation of dye properties. Since Vectashield can be mixed with TRIS-glycerol without impairing its STORM-buffer properties, we also added different chemicals to a 1:4 Vectashield/TRIS-Glycerol solution and assessed their effects on Alexa-647. In particular, we tested three different chemicals: n-Propyl Gallate (NPG), 1,4-diazabicyclo[2.2.2]octane (DABCO), and alpha-Lipoic Acid ( $\alpha$ -LA), all of which had been previously demonstrated to influence the properties of fluorescent dyes [22, 23]. The effects of these chemicals on the STORM buffer properties are summarized in Fig. 5.

Figure 5(A) shows that addition of 1% NPG (w/v) to the Vectashield/TRIS-Glycerol mixture increased the number of photons per molecules, thus making it an attractive chemical to increase the localization precision in this buffer. Addition of 20 mM DABCO (Fig. 5(B)) or 10 mM  $\alpha$ -LA (Fig. 5(C)) did not perturb Alexa-647 blinking, though the brightness of the molecules is slightly decreased. Importantly, none of these chemicals diluted in glycerol can induce blinking when Vectashield is absent in similar imaging conditions. While adding NPG provides an advantage for STORM imaging of Alexa-647 in Vectashield, the other chemicals do

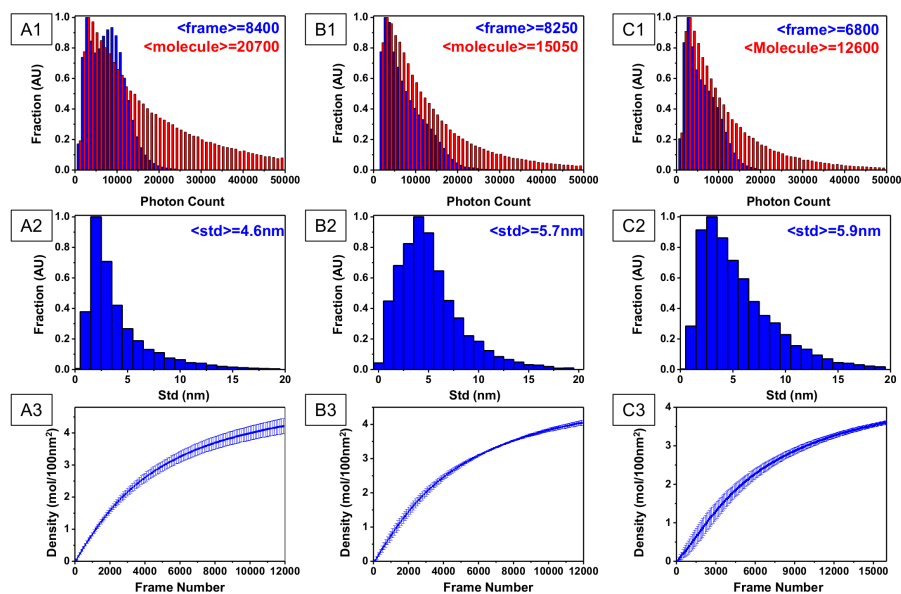


Fig. 5. Statistics on STORM imaging performed in 25% Vectashield - 75% TRIS-Glycerol in which were added 1% NPG (w/v) (A), 20 mM DABCO (B), and 10 mM Lipoic Acid (C). The different panels represent: (1) photon count distribution per frame and per molecule, averaged over three datasets, (2) standard deviation of multiple localizations giving a measure of the frame localization precision, and (3) Density of molecules as a function of number of recorded frames, averaged over three measurements, with error bars indicating the standard deviation.

not, but since they do not prevent Alexa-647 from blinking properly, they provide an promising means to improve multicolor imaging (assessed in Section 3.3).

### 3.2. 3D imaging

STORM imaging is usually performed using high numerical aperture (NA) oil-immersion objectives, to maximize both detection efficiency and localization precision (which scales as  $1/NA$  [20]). An important issue arising from the use of these objectives is that the index mismatch between the buffer and the coverslip can be very large, which leads to strong optical aberrations (mostly defocus and spherical aberrations) that reduce the 3D resolution. We measured the optical index of Vectashield at 590 nm to be  $\approx 1.45$ , which is equal to the highest value reported value for STORM buffers and makes 3D imaging of thick samples much more straightforward [18].

We performed 3D-STORM imaging by adding an astigmatic lens in our detection path, and used the ellipticity of the measured spots to determine the z-position of each detected molecule [17, 18] (see Section 2.3 for more details). Figure 6 shows a 3D-STORM image of microtubules immunostained with Alexa-647 imaged in a mixture of 25% Vectashield-75% TRIS-Glycerol (which also has an index of refraction of  $\approx 1.45$ ), where the depth information is color-coded. We quantified the axial resolution in Fig. 6(B1) by fitting the axial profile of a straight section of microtubule over 200 nm with a Gaussian function, and obtained a full-width at half maximum (FWHM) of 74 nm. Since the nano-structure of microtubules is known, we can deconvolve from this value the size of microtubules, and estimate our axial resolution as  $\approx 40$ -50 nm. Moreover, we can see from the criss-crossing microtubules shown in Fig. 6(B2)

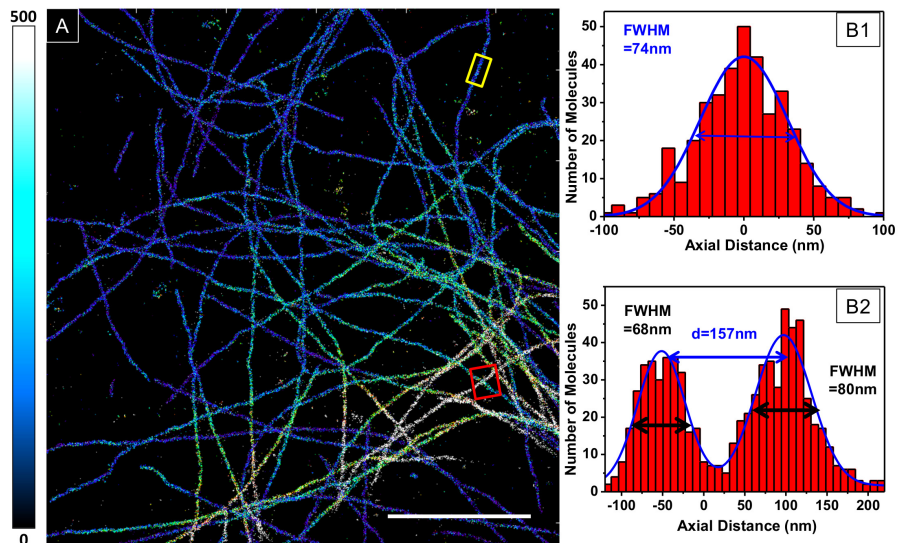


Fig. 6. 3D STORM of Alexa-647-labeled microtubules in Vectashield: (A) Imaging performed in 25% Vectashield-75 % TRIS-Glycerol, scale-bar = 5  $\mu\text{m}$ . (B1&2): axial profile taken from the two regions delimited in A (yellow for (B1), showing a single microtubule; red for (B2) showing two well-resolved microtubules crossing at a distance of  $\approx 160$  nm).

that aberrations due to the index mismatch do not significantly degrade the resolution over several hundreds of nanometers in depth, as the size of the furthest microtubule from the coverslip is not so different from the one closest. Vectashield is therefore well suited for 3D STORM imaging; importantly this is not limited to 3D using astigmatism, and other 3D methods such as biplane imaging [24] or interferometric imaging [25] can benefit from using this buffer.

Although Vectashield - either pure or mixed with TRIS-Glycerol - is well suited for 3D-STORM imaging, there is still a small index mismatch (1.45 vs 1.51) that can affect the resolution. Since we have shown that Vectashield could be diluted in Glycerol and still induce blinking, we further tested its properties when mixing with two different solvents to improve index-matching: PBS and Thiodiglycol (2,2-thiodiethanol or TDE). TDE has a high index of refraction, making it attractive to index-match oil objectives [26].

The optical index of a TDE + Vectashield mixture as a function of Vectashield concentration measured at 590 nm (Fig. 7(A) - blue curve) shows a linear dependence with values ranging from 1.45 to 1.52. We tested a mixture of 25% Vectashield + 75% TDE, which has an optical index of 1.50, for STORM imaging. As can be seen in Figs. 7(B) and 7(C), good blinking was obtained with a high average number of photons per molecule ( $\geq 20,000$ ), and a high enough density to reconstruct a good STORM image of microtubules.

Since PBS is water-based, it can be used to decrease the index of refraction from 1.45 to 1.33 in a linear fashion, as shown in Fig. 7(A) (red curve). There are two interesting values for the index of refraction in the PBS and Vectashield mixture: the first one is 1.33 which is index-matched to water objectives, but would require very low concentrations of Vectashield; moreover, the typical buffers (Thiol + oxygen scavenger) are water-based and thus better candidates for optimal index-matching. The second interesting value is 1.40, which is matched to silicon-oil objectives, and correspond to a 50% Vectashield - 50% PBS mix. We therefore tested this buffer for STORM imaging, and again found that it performed well (Fig. 7(D)), although the photon count is slightly lower than with TRIS-Glycerol or TDE as a solvent (Fig. 7(E)).

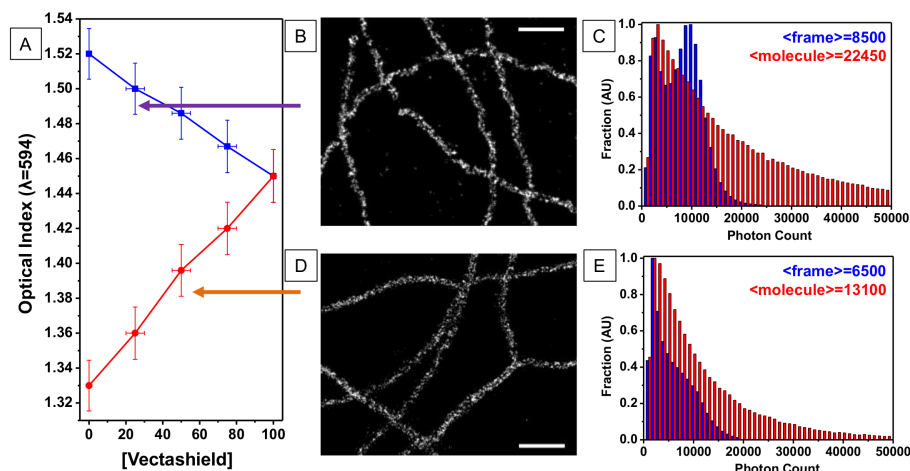


Fig. 7. (A) Index matching with Vectashield: Optical index as a function of Vectashield concentration starting from PBS (red) or TDE (blue), and imaging performed at  $n = 1.5$  (adapted to oil objectives) and  $n=1.4$  (adapted to glycerol objectives) (B-D) STORM imaging of microtubules immunostained with Alexa-647 for the 25% Vectashield-75% TDE buffer and 50% Vectashield - 50% PBS buffer respectively, scale-bar = 500 nm (C-E): photon count distribution per frame and per molecule, averaged over three datasets for the 25% Vectashield-75% TDE buffer and 50% Vectashield - 50% PBS buffer respectively.

The ability to control the optical index of the buffer by mixing Vectashield with different solvents should enable significant improvements in 3D imaging, since the influence of index mismatch on axial localization does not have to be compensated by software, but can instead be corrected directly by properly formulating the buffer.

### 3.3. Multicolor imaging

Multicolor imaging is often required for biological experiments, but the buffers currently used are optimized for Alexa-647 or its close structural analogue Cy5. Although they can still be used with some other dyes [9, 21], the quality of the images obtained with these dyes is much lower [21]. We therefore tested Vectashield on several spectrally distinct dyes to see if we could induce their blinking. The results are summarized in Table 1.

The two dyes tested with peak emission in the green region of the spectrum (excited at  $\lambda = 488$  nm) displayed almost no blinking, while in the orange part of the spectrum (excited at  $\lambda = 532$  nm), Alexa-532 displayed weak blinking that was insufficient to reconstruct a good image in pure Vectashield, but might be promising for a slightly modified mixture. The same can be said for dyes with peak emission in the red part of the spectrum (excited at  $\lambda = 561$  nm) for three Cyanide dyes: Cy3, Cy3.5 and Cy3B, which showed some blinking, whereas Alexa-546, Alexa-568 and Rhodamine6-G did not. Flip-565, a dye that has been engineered to switch independently of the chemical environment [27] did blink a little, but not as well as in PBS. The best dye we identified in the red region of the spectrum is Alexa-555, which could be used to reconstruct a STORM image. However, we found that at Vectashield concentrations higher than  $\approx 20\%$  in TRIS-Glycerol, Alexa-555 became too stable (using a laser power of  $\approx 1 \text{ kW} \cdot \text{cm}^{-2}$ ) at 561 nm which was the maximum that we could obtain on our setup) thus preventing proper STORM imaging. Therefore, a 20% Vectashield-80% TRIS-Glycerol mixture makes an adequate buffer for two-color STORM imaging using Alexa-555 and Alexa-647. Interestingly, when testing whether Cy3 blinking could be improved by the addition of other chemicals

Table 1. Screening of Other Dyes in Pure Vectashield (Except When Explicitly Stated) Performed by Imaging Antibody Stained-Microtubules and Assessing the Quality of the Images Obtained\*

Color (em.)	Dye	Blinking	Comment	
Green	Alexa-488	-		
Green	CF-488	-		
Orange	Alexa-532	+	Excitation $\lambda = 532\text{nm}$	
Red	Cy3	+	Blinking can be improved (Fig. 8)	
Red	Cy3B	+		
Red	Cy3.5	+		
Red	Alexa-546	-		
Red	Alexa-555	++		10-20% Vectashield
Red	Alexa-568	-		
Red	Flip-565	+		Invisible in Widefield
Red	Rhodamine-6G	-		Excitation wavelength far from peak
Far-Red	Alexa-647	+++	See section 3.1	
Far-Red	CF-647	+++	See Fig. 9	
Far-Red	Cy5	++	See Fig. 9	
Far-Red	Dy-647	+++	See section 3.1	
Far-Red	Atto 655	-		
Far-Red	Alexa 700	++	Excitation $\lambda = 641\text{nm}$	

\*Dyes are arranged by their color, and rated on a 1–4 qualitative scale (“-” = no blinking, “+” = some blinking, “++” = blinking allowing the reconstruction of a STORM image, “+++” = blinking comparable to Alexa-647 in previously reported buffer).

or varying Vectashield concentrations, we found that a buffer made of 40% Vectashield/TRIS-glycerol containing 1% NPG (w/v) and 20 mM DABCO significantly improved the blinking of Cy3 and yielded a good STORM image (Fig. 8).

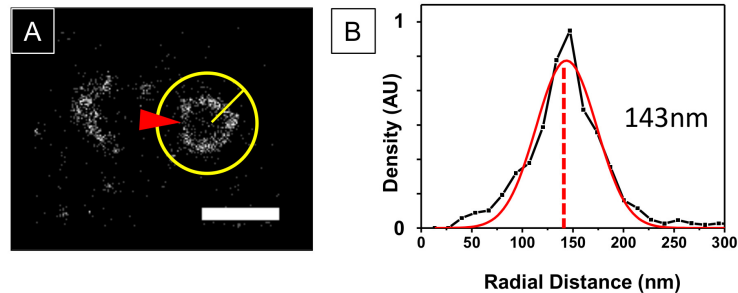


Fig. 8. (A) STORM image of CEP-152 stained with Cy3 using a buffer 40% Vectashield + 1% NPG + 20 mM DABCO, which improves the quality of Cy3 blinking. Scale-bar = 500 nm (B) Radial intensity distribution measured from the yellow ROI defined in (A), and Lorentzian fit showing a peak at  $r = 143\text{ nm}$ .

We went on to test this improved buffer for Cy3 on the centrosomal protein Cep-152. The centrosome is made of two barrel-shaped organelles called centrioles, and Cep-152 localizes at the proximal part of the centrioles [28], forming a  $\approx 300\text{ nm}$  wide ring. We immunostained CEP-152 with rabbit primary and Cy3-conjugated secondary antibodies (see Section 2.2 for more details), and tested STORM imaging in this improved buffer. We obtained a better

blinking than in pure Vectashield, and were able to reconstruct a high resolution STORM image of the ring organization of this protein (Fig. 8(A)). From this image, we measured the radius of the ring by fitting a Lorentzian function to the radial distribution of peaks, and obtained a diameter of  $\approx 300$  nm. This radius is in line with previously measured radii (215 nm [29]), some variability being expected since a different antibody targeting different epitopes was used. We also note that we can see a small gap in the ring structure (red arrowhead in Fig. 8(A)), which is also consistent with previous observations [29]. Since Alexa-647 also blinks in this buffer, it can be used for two-color STORM imaging.

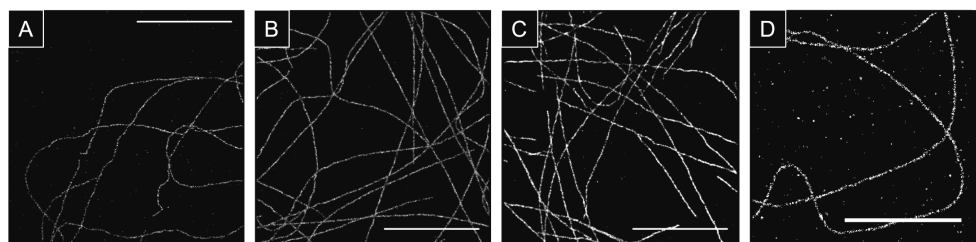


Fig. 9. STORM images obtained with the other working dyes (A) Alexa-555 in 20% Vectashield-80% TRIS-Glycerol (B) Cy-5 (C) CF-647 (D) Alexa-700, all in pure Vectashield. scale-bar = 5  $\mu$ m.

Most of the far-red dyes that we tested (with the exception of Atto-655) blinked very well in Vectashield, which could be related to their similar chemical structure [30]. We also found that Cy5 emitted fewer photons than the other dyes, though still enough to reconstruct a good quality STORM image, while CF-647 displayed very limited photobleaching, and could be imaged for a very large number of frames. Finally, Alexa-700, which has already been used for two color STORM imaging [31], blinked in Vectashield even when excited with a 641 nm laser, but the number of detected photons per molecule was almost ten times lower than what is achieved with Alexa-647. This is in part due to the use of non-adapted emission filters and excitation wavelength. We show in Fig. 9 representative STORM images of microtubules stained with the different dyes rated “++” or “+++” in Table 1. Though none of them is better than Alexa-647 in pure Vectashield, they provide adequate blinking and can be used for multicolor imaging. Moreover, the ability to add different chemicals and improve their blinking provides an exciting perspective.

#### 4. Conclusion and outlook

Vectashield provides a simple yet powerful buffer for 3D-STORM, which should simplify the access to this high-resolution method. In addition to its simplicity, using Vectashield for STORM microscopy provides several advantages over existing schemes. For example, reproducibility is much higher than with the other commonly used buffers, whose compositions differ between publications (concentrations, pH) without a clear explanation of how the conditions were optimized in each case. In particular, the absence of enzymatic oxygen scavenger system here significantly reduces the variability, since the most commonly used system results in a time-dependent acidification of the buffer [10] which can adversely affect the photophysics of dyes [11]. Moreover this lack of enzymes allows imaging in Vectashield to be performed over very long periods of time. Since Vectashield also preserves samples, a sample mounted in Vectashield can be kept at 4°C and imaged up to several weeks after preparation, even allowing repeated measurements on the same sample.

In terms of 3D imaging, the intrinsically high index of refraction of Vectashield makes it very well suited to provide better index-matching than water-based buffers, and this can further be improved by mixing it with TDE resulting in an almost perfectly index-matched buffer. We identified two different multicolor combination (Alexa-555/Alexa-647 and Cy3-Alexa647) that used two different buffer compositions, and we expect that screening more dyes and more chemicals will provide improved combinations.

We stress that all the imaging presented here was performed with a moderate NA objective (NA = 1.3), and using the conventional CCD converter of the EMCCD camera, which means that 2D resolutions down to 10-20 nm can be obtained on a simple inexpensive setup. Since Vectashield can also be used in 3D-SIM microscopy, one potential perspective would be to combine SIM and STORM for multicolor imaging, for example with blue and green fluorophores used for SIM (as low wavelengths yield the highest resolution in SIM), and red plus far-red dyes used for STORM (as they exhibit better blinking in the buffers reported so far, including Vectashield). This would be relatively straightforward since both are based on wide-field microscopes.

### **Acknowledgments**

We thank Harald Hess for the use of Peakselector, Thomas Pengo for discussions and comments, Lina Carlini for help with the spectral measurements, Lada Sycheva et Petr Leiman for the use of the fluorometer, Kai Johnson & Grazvydas Lukinavicius for the SNAP-EB3 plasmid and BG-Dy647, and Carine Ben Adiba for the conjugated  $\alpha$ -Tubulin-Cy3B antibodies. N.O. and S.M. received funding from the ERC (243016-PALMassembly), D.K. from the Swiss Cancer League (grants 02024-2007 and 02584-02-2010 to P.G.).